Optical detection of Eu^{3+} sites in $LiNbO_3$:Eu^{3+} and $LiNbO_3$:MgO:Eu^{3+}

J.E. Muñoz Santiuste,* B. Macalik,† and J. García Solé
Departamento de Física de Materiales C-IV, Universidad Autónoma de Madrid, Cantoblanco 28049 Madrid, Spain
(Received 17 June 1992)

The fluorescence of Eu^{3+} in $LiNbO_3$ has been investigated using laser-excited site-selection spectroscopy. Four different crystal-field sites, denoted as Eu(1), Eu(2), Eu(3), and Eu(4), have been detected and optically characterized through their corresponding $^5D_0 \rightarrow {}^7F_1$ magnetic-dipole emission transitions. The local symmetry of the Eu^{3+} ions in these sites deviates slightly from the C_3 main symmetry as a consequence of distortions perpendicular to the c ferroelectric axis. The relative concentrations of these sites have been studied as a function of the [Li]/[Nb] concentration ratio. It is suggested that the formation of $Eu^{3+}(Nb^{5+})$-$Eu^{3+}(Li^+)$ pairs is responsible for the major Eu(3) and Eu(4) sites, while the Eu(1) and Eu(2) sites correspond to Eu^{3+} ions in Nb^{5+} lattice positions but perturbed by different charge compensating defects. The effect of codoping with Mg^{2+} ions has also been investigated; the same Eu^{3+} sites as in the singly doped system are present, although the Eu(1) site is strongly enhanced in relation to the others.

I. INTRODUCTION

Lithium niobate is a relevant material because of its several optoelectronic applications, as optical waveguide substrata,[1] photorefractive devices,[2] and self-frequency doubled and self-Q-switched solid-state lasers.[3–6] In these devices dopant (transition or rare earth) ions have to be introduced either during the crystal growth or by ion implantation. The determination of the different impurity sites as well as its local symmetry are essential for a complete understanding of the physical properties related to the applications referred to above.

Site selection spectroscopy has proved to be a very useful technique in determining the different impurity sites in $LiNbO_3$:Nd^{3+} (Ref. 7–9) and $LiNbO_3$:Cr^{3+}.[9–11] This technique permits selective excitation of ions in specific types of crystal-field sites and allows to distinguish between dopant ions in different local environments (sites). It is important to remark that the term "site" is commonly used for an ion in a specific crystal field. Thus we can have different sites even for ions in the same lattice positions.

Eu^{3+} is a particularly suitable ion for site selection spectroscopy because of the sensitivity of its energy levels to the crystal environment. The crystal-field level structure has been determined in $LiNbO_3$:Eu^{3+} crystals based on the optical absorption spectra.[12] Three possible lattice positions are available for the cation impurity ions according to the structure of $LiNbO_3$: Li^+, Nb^{5+}, and structural vacancy. Each of these sites is surrounded by six O^{2-} ions distributed in two triangles (up and down) along the c ferroelectric axis. The experimental results have shown that the various absorption and emission bands are split in two components.[12–14] These components in the optical bands were interpreted as a consequence of the presence of two nonequivalent Eu^{3+} sites in C_3 symmetry.[12,13] These sites were associated with the Li^+ and Nb^{5+} lattice positions. The optical characterization of these two Eu^{3+} sites was carried out by studying the relative contribution of the two components in the $^7F_0 \rightarrow {}^5D_2$ absorption spectrum as a function of the [Li]/[Nb] concentration ratio.[14] The occupation of these lattice positions has been confirmed by means of Rutherford backscattering (RBS) channeling technique.[15] These measurements have shown that Eu^{3+} ion occupies only Li^+ and Nb^{5+} lattice positions, not the intrinsic vacancy one.

In this paper laser-excited site-selection spectroscopy has been used to explore the possibility of the formation of Eu^{3+} sites not previously detected by the standard optical techniques. In fact, the formation of other Eu^{3+} luminescent centers has been reported to occur in nonstoichiometric crystals although these centers could not be resolved in the Eu^{3+} emission spectrum.[16] Moreover the first results reported up to now under narrow-band laser excitation have shown additional structure in the emission spectrum of Eu^{3+},[17] suggesting the formation of more than two Eu^{3+} sites. Therefore, the structure in the emission spectrum needs to be investigated in more detail. For this purpose $LiNbO_3$:Eu^{3+} crystals with three different stoichiometries ([Li]/[Nb] concentration ratio in melt) have been used.

The experimental results reveal the presence of, at least, four Eu^{3+} crystal-field sites, which can be labeled through the $^5D_0(A) \rightarrow {}^7F_1(A)$ emission bands of Eu^{3+}. In addition, the structure observed in the $^5D_0(A) \rightarrow {}^7F_1(E)$ emission of each Eu^{3+} site reveals that the symmetry is lower than C_3. This reduction of the C_3 symmetry must be a consequence of the proximity of charge compensating defects close to each type of Eu^{3+} center. The evolution of the relative concentration of these sites with the [Li]/[Nb] concentration ratio permits us to elucidate on its nature.

Finally, the effects of codoping with Mg^{2+} ions on the

optical bands of each Eu^{3+} site have also been investigated. The interest of this research is that the addition of 4.5% or more of Mg^{2+} to the $LiNbO_3$ crystal produces a strong reduction in the photorefractive effect[18] so that the laser damage is reduced. On the other hand, codoping with Mg^{2+} ions could produce new sites for the Eu^{3+} ions, as reported for $LiNbO_3$:MgO:Nd^{3+} (Refs. 7–9) and $LiNbO_3$:MgO:Cr^{3+}.[9,11] However, the experimental results obtained in $LiNbO_3$:MgO:Eu^{3+} have shown that only a redistribution of Eu^{3+} sites is produced, while no new Eu^{3+} sites are detected.

II. MATERIAL AND EXPERIMENTAL TECHNIQUES

Europium-doped $LiNbO_3$ crystals were grown in our laboratory by the Czochralski method from grade I Johnson-Mathey powder. 1 mol % of Eu^{3+} (0.5% of Eu_2O_3) was added to a stoichiometric ([Li]/[Nb]=1), a congruent ([Li]/[Nb]=0.94) and a niobium rich ([Li]/[Nb]=0.88) melts. The MgO codoped crystal was grown from a congruent melt with a 0.5 mol % of Eu_2O_3 and a 6% of MgO. These europium dopant concentrations are lower than the limit of solubility[16] and so the formation of second Eu-precipitated phases is not expected.

The green line of a Nd:YAG (where YAG is yttrium aluminum garnet) laser (532 nm) was used as an excitation source for comparative emission measurements between crystals with different stoichiometries. Site-selection excitation was achieved using Coumarine 460 as a dye in a EG&G 2100 tunable dye laser. The excitation width was ~0.15 nm. The luminescence was dispersed by a Spex 500M monochromator (spectral resolution ~0.05 nm) and detected by a cooled Hamamatsu R4929 photomultiplier. The signals were recorded using a SR400 two-channel gated photon counter. Decay time measurements were performed under dye laser excitation using the average facilities of a Tektronix 2440 digital storage oscilloscope. Samples were mounted in a temperature-controlled closed-cycle Leybold He cryostat for low-temperature (15 and 100 K) measurements.

III. EXPERIMENTAL RESULTS

The optical absorption spectrum of Eu^{3+} (visible region) in $LiNbO_3$ consists of a great number of bands associated with transitions from the lower Stark levels ($^7F_0$ to $^7F_5$) of the ^7F ground-state multiplet up to Stark levels of the $^5D_0$, $^5D_1$, and $^5D_2$ excited state multiplets.[13] In addition, several absorption bands appear split because of the presence of two nonequivalent Eu^{3+} sites in C_3 symmetry: Eu^{3+} replacing Li^+ and Nb^{5+} lattice sites.[12–14]

Figure 1 shows the 100-K emission spectrum of a congruent $LiNbO_3$:Eu^{3+} sample, in the wavelength range from 580 to 640 nm, under excitation with the green line of a Nd:YAG laser (532 nm). In this wavelength range the most prominent emission bands are present.[13] The spectrum consists of four bands, with different levels of structure, which correspond (in order of increasing

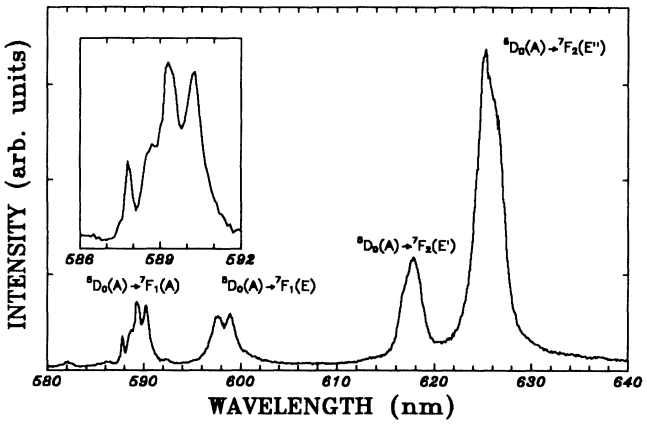

FIG. 1. Emission spectrum of Eu^{3+} for a congruent $LiNbO_3$:Eu^{3+} crystal excited at 532 nm at 100 K. Inset shows the $^5D_0(A) \rightarrow {}^7F_1(A)$ emission band magnified.

wavelengths) to the $^5D_0(A) \rightarrow {}^7F_1(A)$, $^7F_1(E)$, $^7F_2(E')$, and $^7F_2(E'')$ transitions of Eu^{3+} in C_3 symmetry. The emission spectrum excited at this laser wavelength disappears at lower temperatures because light at 532 nm is not absorbed. This excitation (absorption) wavelength corresponds to the $^7F_1(A) \rightarrow {}^5D_1(E)$ transition and, at low temperature, the $^7F_1(A)$ ground state is not thermally populated.

Inspection of Fig. 1 shows that the better resolution for the structure is in the $^5D_0(A) \rightarrow {}^7F_1(A)$ emission. This emission band consists of four peaks (see inset) at 587.8, 588.7, 589.3, and 590.3 nm. Since the degeneracy of the ground and the excited levels is equal to 1, these four peaks indicate the presence of four Eu^{3+} crystal-field sites. Hereafter these sites (peaks) will be denoted as Eu(1) (587.8 nm), Eu(2) (588.7 nm), Eu(3) (589.3 nm), and Eu(4) (590.3 nm). In order to gain an insight into the location and relative concentration of these Eu^{3+} centers (sites) in the $LiNbO_3$ matrix, a more detailed study of this emission band becomes necessary.

Figure 2 shows the $^5D_0(A) \rightarrow {}^7F_1(A)$ structured emission spectra for three $LiNbO_3$ crystals with different [Li]/[Nb] concentration ratios. The same four peaks (sites) as in the congruent sample (see Fig. 1) are present in every crystal. The emission spectra were fitted by adding the contribution of the same four Gaussian bands. Notice that the relative intensities of these peaks change with the [Li]/[Nb] concentration ratio, indicating that the relative concentration of each Eu^{3+} site depends on the crystal stoichiometry ([Li]/[Nb] concentration ratio into the melt). In addition it should be noted how, on going towards a less stoichiometric composition (lower [Li]/[Nb] concentration ratio), the emission lines are broadened, indicating that the crystal is becoming more inhomogeneous. Anyhow, even in the near stoichiometric crystal ([Li]/[Nb]=1 in the melt), the emission lines are still broad ($\gtrsim$ 18 cm^{-1} full width at half maximum) compared to the typical homogeneous linewidths of Eu^{3+} in a single crystal as, for instance, Gd_2O_3:Eu^{3+} (2 cm^{-1}).[19] This fact justifies the Gaussian shape used for the emission band of each europium site.

Figure 3 shows the dependence of the emission intensity (measured as the total area under each band) on the [Li]/[Nb] concentration ratio for each Eu^{3+} site. The highest peaks, Eu(3) and Eu(4), increase its intensity together with the [Li]/[Nb] concentration ratio, while the intensity of those of Eu(1) and Eu(2) peaks decrease.

Site-selection experiments were carried out under tunable dye laser excitation in the spectral region of the $^7F_0(A) \rightarrow {}^5D_2(E'')$ and $^7F_0(A) \rightarrow {}^5D_2(E')$ absorption bands. These absorption bands are the highest in the absorption spectrum[13] and both show a doublet structure due to the Eu^{3+} sites. These two sites were correlated to the $Eu^{3+}(Nb^{5+})$ and $Eu^{3+}(Li^+)$ regular lattice sites.[12–14] However, the results here obtained by fine resolution fluorescence measurements indicate that at least four Eu^{3+} different sites are present.

Figure 4(a) shows, as an illustrative example, a series of four site-selective emission spectra obtained for a congruent sample by tuning the dye laser through the $^7F_0(A) \rightarrow {}^5D_2(E'')$ absorption band. This absorption consists of two bands which have been associated with the $Eu^{3+}(Nb^{5+})$ and $Eu^{3+}(Li^+)$ sites in order of increasing wavelength.[13] For the sake of clarity this absorption band has been displayed in Fig. 4(b), where the excitation wavelengths used in Fig. 4(a) have been indicated by arrows. These excitation wavelengths correspond to the best conditions in order to selectively excite each Eu^{3+} site. Thus the $^5D_0(A) \rightarrow {}^7F_1(A)$ emission line of each site appears maximized in relation to the other sites. It is important to note that the Eu(1), Eu(2), and Eu(3) sites are mainly excited in the absorption band of $Eu^{3+}(Nb^{5+})$ site while the Eu(4) site is excited in the absorption band of $Eu^{3+}(Li^+)$ site.

In Fig. 4(a) the spectral region corresponding to the $^5D_0(A) \rightarrow {}^7F_1(E)$ emission transition is also included for each Eu^{3+} site. It is important to note that the doublet structure appearing in this band is not due to different Eu^{3+} sites, because the relative intensity of these two components is practically independent of the excitation wavelength. Therefore this doublet structure must be a consequence of a deviation from the C_3 symmetry for each Eu^{3+} site. This deviation reduces the C_3 local symmetry and the ground level, which is doubly degenerated, splits into two levels. Therefore the amount of this splitting is a rough measure of the magnitude of the reduction in the C_3 symmetry. These values together with the corresponding $^5D_0(A) \rightarrow {}^7F_1(E)$ emission peak position for each europium site are included in Table I. It should be noted that the splitting in the $^7F_1(E)$ level is very similar for the Eu(1), Eu(2), and Eu(3) sites, while it is reduced in the Eu(4) site.

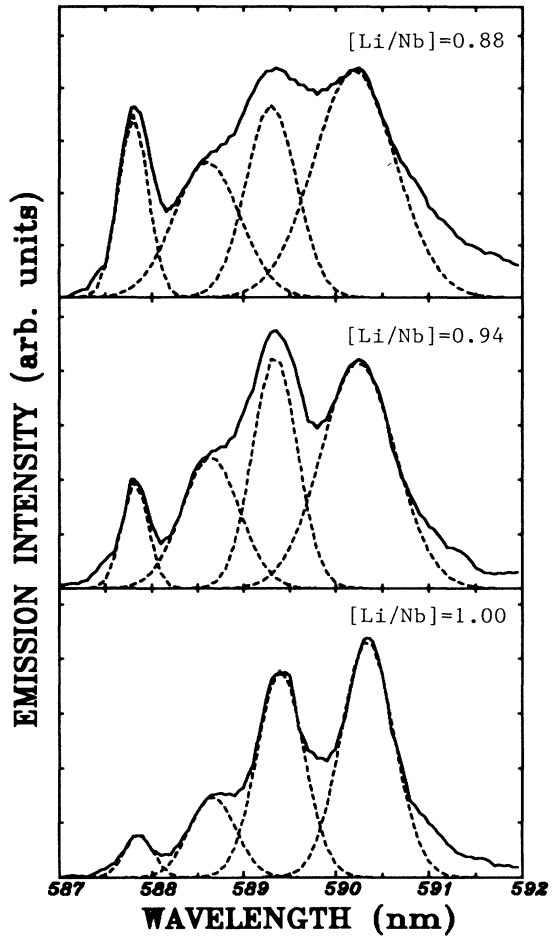

FIG. 2. $^5D_0(A) \rightarrow {}^7F_1(A)$ emission spectra of Eu^{3+} for three $LiNbO_3$:Eu^{3+} crystals with different [Li]/[Nb] concentration ratios. Excitation wavelength 532 nm, T=100 K. Best fitting, obtained with four Gaussian bands, is represented with dotted lines.

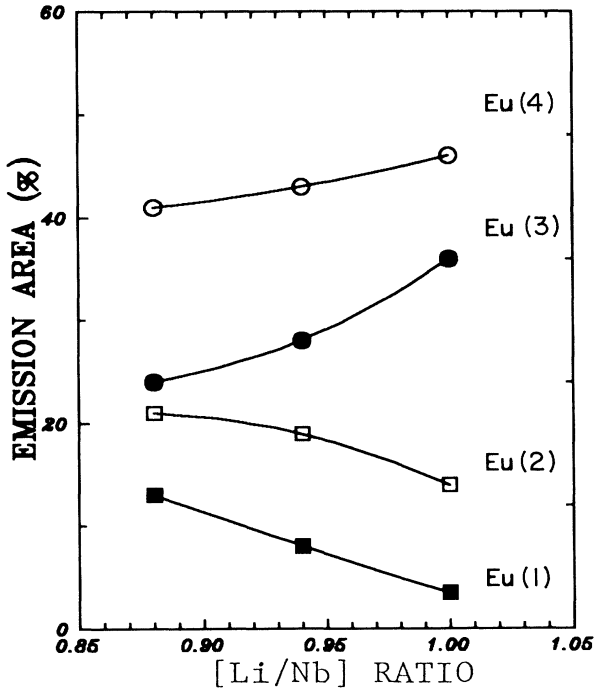

FIG. 3. $^5D_0(A) \rightarrow {}^7F_1(A)$ emission area of the Eu^{3+} peak showed in Fig. 2 as a function of [Li]/[Nb] concentration ratio.

Now, taking advantage of the site selection spectroscopy, decay time measurements can be performed in the emission spectrum of each Eu^{3+} site. Decay time plots show an exponential behavior including a small short component (τ<20 μs) that appears as a consequence of transfer between Eu^{3+} ions. This transfer has been shown to be possible even at long (>50 Å) distances between the Eu^{3+} ions.[17] Each Eu^{3+} site presents a defined $^5D_0$ lifetime which can also be used for its optical characterization. The lifetime values obtained (included in Table I) are consistent with both magnetic and electric dipole emission transitions from this ($^5D_0$) level.

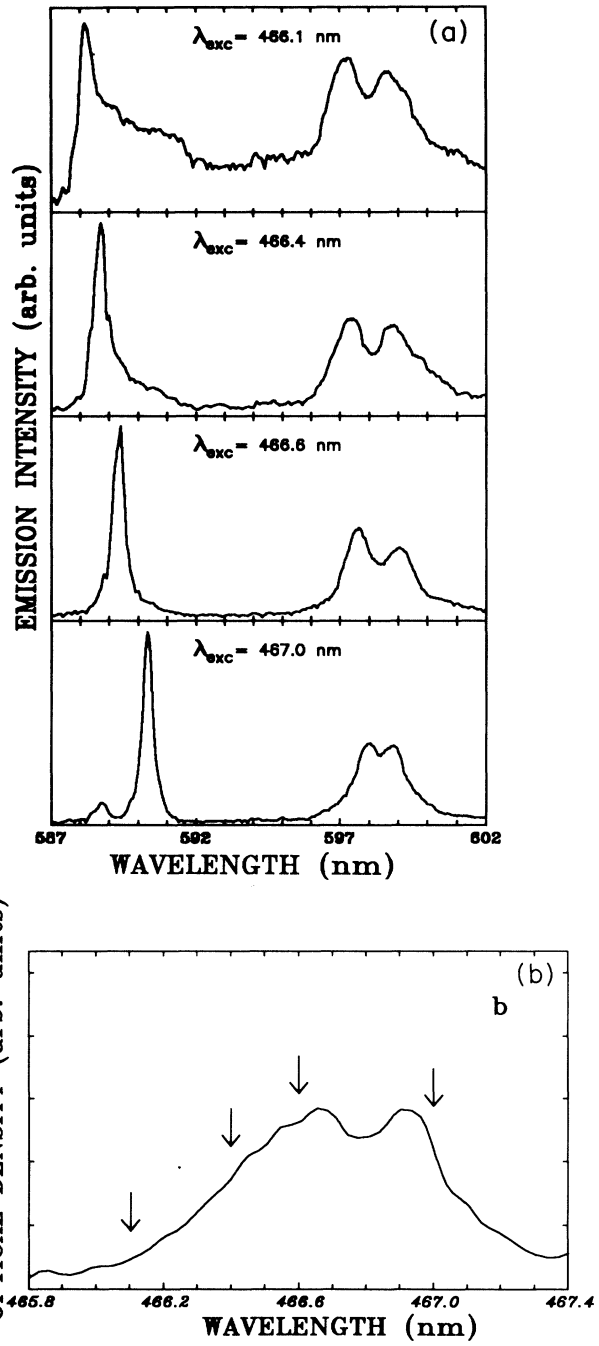

FIG. 4. (a) 15-K emission spectra ($^5D_0 \rightarrow {}^7F_1$ transitions) of a congruent sample obtained under four different narrow laser excitation wavelengths, in the spectral region of the $^7F_0(A) \rightarrow {}^5D_2(E'')$ transition for Eu^{3+} ion. (b) Absorption spectrum corresponding to this sample in the $^7F_0(A) \rightarrow {}^5D_2(E'')$ transition. Excitation wavelengths used in (a) are indicated by arrows.

TABLE I. Summary of spectroscopic data obtained for the different Eu^{3+} sites in $LiNbO_3$:Eu^{3+}.

Site	$^5D_0(A) \rightarrow {}^7F_1(A)$ (nm)	Splitting on the $^7F_1(E)$ level (cm^{-1})	τ ($^5D_0$) (μs)
Eu(1)	587.8	39	940
Eu(2)	588.7	43	700
Eu(3)	589.3	41	600
Eu(4)	590.3	25	580

Once the four europium sites appearing in $LiNbO_3$:Eu^{3+} have been optically characterized, the effect of codoping with Mg^{2+} ions can be investigated. Figure 5 shows the $^5D_0(A) \rightarrow {}^7F_1(A)$ emission spectrum of a congruent crystal of $LiNbO_3$:Eu^{3+} codoped with a 6% of MgO. The same peaks (europium sites) as in the singly doped (only with Eu^{3+}) crystal are present. This assertion was verified by means of site selection on each site. However the emission band associated with the Eu(1) site appears clearly magnified with respect to the other sites. In addition, the emission spectrum of the doubly doped crystal (Fig. 5) is broader than that obtained for the singly doped crystals (Fig. 2), i.e., the doubly doped crystal becomes much more inhomogeneous. Thus the main effect of codoping with Mg^{2+} ions is to favor the formation of the Eu(1) center. It is important to say that the amount of europium incorporated into the doubly doped crystal is reduced. Moreover there is not any evidence for the formation of new centers. The formation of M^{3+}-Mg^{2+} mixed centers (M being the optically active center) was reported to occur in the $LiNbO_3$:MgO crys-

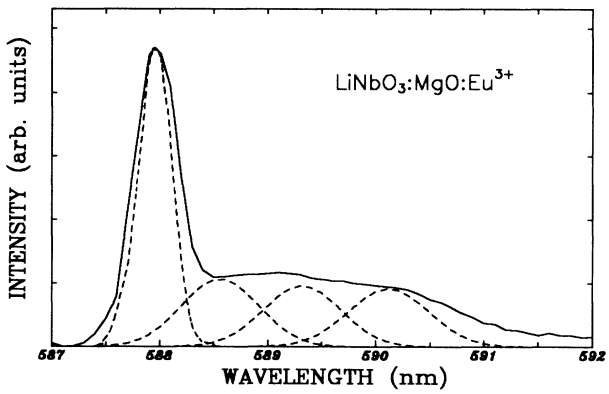

FIG. 5. $^5D_0(A) \rightarrow {}^7F_1(A)$ emission spectrum of Eu^{3+} obtained at 100 K for a congruent $LiNbO_3$:MgO:Eu^{3+} crystal under excitation at 532 nm. The same four Gaussian bands as in Fig. 2 are used to fit the emission spectrum.

tals codoped with Nd^{3+} (Refs. 7–9) or with Cr^{3+} (Refs. 9–11) ions. The nonexistence of those kinds of centers in the $LiNbO_3$:Eu^{3+} system was also corroborated by examining the infrared OH^- absorption region. When mixed centers are formed a new IR absorption band appears as a consequence of a M^{3+}-OH^--Mg^{2+} association which produces a new OH^- vibration.[20] It was not the case of the $LiNbO_3$:Mg^{2+}:Eu^{3+} in which no new IR absorption bands of OH^- were found, indicating that no mixed centers are formed in this system.

IV. DISCUSSION

From the experimental results reported in this work, the presence of, at least, four nonequivalent (different crystal field) Eu^{3+} sites in europium doped lithium niobate is clear. These sites have been labeled as Eu(1), Eu(2), Eu(3), and Eu(4). Because only Li^+ or Nb^{5+} lattice positions are occupied,[15] these crystal-field sites have to be thought of for ions located only in Li^+ or Nb^{5+} lattice positions, but in different local environments. Therefore the spectroscopic data have to be analyzed by considering this four Eu^{3+} sites instead of the two sites reported by optical absorption measurements.[12–14] These four europium sites can be characterized by their corresponding ${}^5D_0(A) \rightarrow {}^7F_1(A)$ emission lines.

In addition, the structure observed in the ${}^5D_0(A) \rightarrow {}^7F_1(E)$ transition is due to crystal-field splitting in the ${}^7F_1(E)$ level of Eu^{3+} in each site. Therefore this splitting indicates that the local symmetry of Eu^{3+} ion is lower than C_3 for each site. Local charge compensating defects have to be considered for each Eu^{3+} site to account for this reduction in the local symmetry. The presence of these compensating defects is reasonable because of the Li^+ deficiency in $LiNbO_3$ crystals, even in those crystals grown with the stoichiometric melt composition.[21] In order to decrease the C_3 main symmetry these charge compensating defects cannot be located along the same c axis in which the Eu^{3+} ions are lying. The amount of splitting in the ${}^7F_1(E)$ transition is a rough measure of the deviation from the C_3 symmetry for each Eu^{3+} site. In such a way, the splitting values reported in Table I suggest that the Eu^{3+} ions have a similar local environment [similar ${}^7F_1(E)$ splitting] in the Eu(1), Eu(2), and Eu(3) sites, while in the Eu(4) site the environment is less distorted from the C_3 symmetry. In any case, it seems to be difficult to get information on the nature of Eu^{3+} sites by only considering these small differences in the crystal field.

To gain information about the nature of the europium sites the experimental results on crystals with different stoichiometries represent a useful help. It is well known that in nonstoichiometric samples of $LiNbO_3$ some percentage of the Nb^{5+} ions ($5x$ in formula below) are occupying Li^+ lattice sites, the so called "antisites." Then, in order to maintain charge neutrality, an associated number of Nb^{5+} vacancies ($4x$) are created, according to the formula $[Li_{1-5x}Nb_{5x}]\ Nb_{1-4x}O_3$ with $0 \leq x \leq 0.02$.[21,22] Consequently, the number of Nb^{5+} antisites, and the corresponding number of Nb^{5+} vacancies, decreases when going towards a more stoichiometric composition (higher [Li]/[Nb] concentration ratio). It is expected that an increase in the [Li]/[Nb] concentration ratio lead to a less probable location in Nb^{5+} sites for the Eu^{3+} ions because of the reduction in Nb^{5+} vacancies.[14] In this respect the data reported in Fig. 3 clearly indicate that the relative concentration of Eu(4) and Eu(3) sites increases with the [Li]/[Nb] concentration ratio, while the relative concentrations of Eu(1) and Eu(2) sites decrease.

On the other hand, two additional experimental facts have to be considered before the assignment of the europium sites detected in this work can be made. First, it is reasonable to think that the major ${}^5D_0(A) \rightarrow {}^7F_1(A)$ emission peaks have to be associated with the regular Li^+ and Nb^{5+} lattice sites. Second, previous RBS experimental results performed in congruent $LiNbO_3$:Eu^{3+} crystals have shown that the 64% of Eu^{3+} ions are occupying Nb^{5+} while only 36% are in Li^+ sites.[15] Therefore, most of the Eu^{3+} ions are expected occupying Nb^{5+} sites. Nevertheless, the site occupancy may depend on the [Li]/[Nb] concentration ratio.

At this point, it is possible to make an assignment for the europium sites by taking advantage of the above picture, and considering the excitation wavelengths in which each Eu^{3+} center is mainly excited [see Fig. 4(b)]. Reference to this figure indicates that the Eu(1), Eu(2), and Eu(3) sites are mainly excited in the absorption region of Eu^{3+} ions located in Nb^{5+} positions, while Eu(4) site is mainly excited in the spectral region of Li^+ substitution. Therefore we assign the Eu(1), Eu(2), and Eu(3) sites to three crystal-field sites in which Eu^{3+} ions are occupying Nb^{5+} positions, but in different environments. The Eu(4) site is related to Eu^{3+} ions located at Li^+ lattice sites. This assignment explains the dependence obtained for the relative concentration of the Eu(1), Eu(2), and Eu(4) sites with the [Li]/[Nb] concentration ratio. However, the dependence expected for the Eu(3) site seems to be inconsistent with Nb^{5+} occupation. In fact this peak follows a similar trend to that observed for the Eu(4) site (Eu^{3+} ions in Li^+ positions). This behavior can be explained by considering the formation of $Eu^{3+}(Nb^{5+})$-$Eu^{3+}(Li^+)$ pairs. The two Eu^{3+} ions of these pairs should be considered for the Eu(3) and Eu(4) sites optically detected.

The presence of these pairs appears to be reasonable from the local charge compensation point of view. In addition experimental evidence for the formation of $Cr^{3+}(Nb^{5+})$-$Cr^{3+}(Li^+)$ close dopant ion pairs has been given in $LiNbO_3$:Cr^{3+}.[10] Moreover, shell-model calculations have shown that self-compensation is the preferred mode of incorporation of all types of impurity ions in $LiNbO_3$.[23] In fact, it seems to be the most important mechanism of europium incorporation in $LiNbO_3$:Eu^{3+}.[16] Thus, according to this model, the major sites should be Eu(4)(Li^+) and Eu(3)(Nb^{5+}) sites. Because of the pairing, these Eu^{3+} ions should be in the same concentration and giving optical bands of similar intensities, as experimentally observed. In addition these pairs account for the similar dependence of these Eu(3) and Eu(4) sites with the [Li]/[Nb] concentration ratio (see Fig. 3). According to this scheme all $Eu^{3+}(Li^+)$

ions [Eu(4) sites] are paired with $Eu^{3+}(Nb^{5+})$ ions [Eu(3) sites]. The excess of $Eu^{3+}(Nb^{5+})$ ions are distributed in two different crystal-field sites: Eu(1) and Eu(2). These two sites must correspond to Eu^{3+} ions in Nb^{5+} sites but perturbed by other than europium ions charge compensating defects.

The relative concentration of these two sites [Eu(1) and Eu(2)] decrease with the [Li]/[Nb] concentration ratio (see Fig. 3) because of a parallel decreasing in the available Nb^{5+} vacancies. This decreasing is due to a reduction in the number of Nb^{5+} antisites (Nb^{5+} in Li^+ sites) as a consequence of a less Li^+ defficiency. Therefore a possible charge compensating defect is a Nb^{5+} antisite. This charge compensating defect could account for the Eu(2) centers [two $Eu^{3+}(Nb^{5+})$ ions and one Nb^{5+} antisite for a complete local charge compensation]. On the other hand, the charge compensating defect of Eu^{3+} in the Eu(1) site cannot be associated with the Li^+ deficiency. In fact this Eu(1) site is the predominant one after codoping with Mg^{2+} ions and these ions reduce the common defects associated with Li^+ defficiency.[21,24] A possible model for this Eu(1) site is an oxygen vacancy close to a $Eu^{3+}(Nb^{5+})$ ion. However it is not clear how these vacancies have been incorporated into the $LiNbO_3$ crystal. Moreover the existence or nonexistence of these vacancies is at present a subject of controversy.[21]

Other important result inferred from this work is that the local symmetry is lower than C_3 in all europium sites. It is clear that Eu(3)(Nb^{5+}) and Eu(4)(Li^+) sites locally compensate their charge on each other. These pairs have to be oriented in a direction different from that of the c ferroelectric axis which should explain the lowering of the C_3 symmetry. On the other hand, the charge compensating defects, invoked for the Eu(1) and Eu(2) centers, have to be out of the c axis in which Eu^{3+} ions are located. In any case, an ultimate structure for the Eu^{3+} sites detected in this work cannot be made by only using optical techniques.

V. CONCLUSIONS

Site selection measurements in $LiNbO_3:Eu^{3+}$ have shown the presence of four Eu^{3+} sites instead of the two previously reported. The structure observed in the $^5D_0(A) \rightarrow {}^7F_1(E)$ emission band indicates that in these sites the Eu^{3+} ions are in a local symmetry lower than C_3. This can only be reached as a consequence of perturbations perpendicular to the c ferroelectric axis of the crystal, produced by the proximity of different compensating defects. The formation of $Eu^{3+}(Nb^{5+})$-$Eu^{3+}(Li^+)$ pairs is strongly suggested. Finally, codoping with Mg^{2+} ions the $LiNbO_3:Eu^{3+}$ crystal only produces a redistribution of the same Eu^{3+} sites present in the singly doped system.

ACKNOWLEDGMENTS

The authors would like to acknowledge stimulating discussions with H. Murrieta (UNAM, Mexico D.F.) as well as his critical reading of this manuscript. This work has been supported by the Comisión Asesora de Investigación Científica y Técnica (Spain) under project MAT 93/0130. One of us (B. Macalik) acknowledges financial support from Ministerio de Educación y Ciencia (Spain), which made this work possible.

*Permanent address: Departamento de Ingeniería, Escuela Politécnica Superior, Universidad Carlos III de Madrid, Av. del Mediteráeo 20, Leganés 28913, Madrid, Spain.

†Permanent address: W. Trzebiatowski Institute for Low Temperature and Structure Research, Polish Academy of Sciences, Post Office Box 937, 50-950 Wroclaw, Poland.

[1] M.N. Armenise, C. Canali, E. de Sario, and E. Zanoni, Mater. Chem. Phys. **9**, 267 (1983).

[2] *Photorefractive Materials and Their Applications I*, edited by P. Gunter and J.P. Heingards (Springer-Verlag, Berlin, 1988).

[3] L.F. Johnson and A.A. Ballman, J. Appl. Phys. **40**, 294 (1969).

[4] T.Y. Fan, A. Cordova-Plaza, M.J. Digonnet, R.L. Byer, and H.J. Shaw, J. Opt. Soc. Am. B **13**, 140 (1986).

[5] A. Cordova-Plaza, M.J. Digonnet, and H.J. Shaw, IEEE J. Quantum Electron. **QE-23**, 262 (1987).

[6] E. Lallier, J.P. Pocholle, M. Papuchon, M. de Micheli, M.J. Li, Q. He, D.P. Ostrowsky, G. Crezes-Besnet, and E. Pelletier, Opt. Lett. **15**, 682 (1990).

[7] G. Lifante, F. Cussó, F. Jaque, J.A. Sanz García, A. Monteil, B. Varrel, G. Boulon, and J. García Solé, Chem. Phys. Lett. **176**, 482 (1991).

[8] J.O. Tocho, E. Camarillo, F. Cussó, F. Jaque, and J. García Solé, Solid State Commun. **80**, 575 (1991).

[9] J. García Solé, A. Monteil, G. Boulon, E. Camarillo, J.O. Tocho, I. Vergara, and F. Jaque, J. Phys. (Paris) Colloq. **52**, C7-403 (1991).

[10] Weiyi, Jia, Huimin, Liu, R. Knutson, and W.M. Yen, Phys. Rev. B **41**, 10906 (1989).

[11] E. Camarillo, J. O. Tocho, I. Vergara, E. Dieguez, J. García Solé, and F. Jaque, Phys. Rev. B **45**, 4600 (1992).

[12] L. Arizmendi and J. M. Cabrera, Phys. Rev. B **31**, 7138 (1985).

[13] L. Arizmendi, F. Abella, and J. M. Cabrera, Ferroelectrics **50**, 75 (1984).

[14] B. Macalik, J.A. Sanz García, and J. García Solé, Ferroelectrics Lett. **12**, 123 (1990).

[15] L. Rebouta, J.C. Soares, M.F. Da Silva, J.A. Sanz García, E. Dieguez, and F. Agulló-López, Appl. Phys. Lett. **55**, 120 (1989).

[16] M.E. Villafuerte-Castrejón, A.R. West, and J.O. Rubio, Radiat. Eff. Defects Solids **144**, 175 (1990).

[17] J.K. Timinsky, C.M. Lawson, and R.C. Powel, J. Chem. Phys. **77**(a), 4318 (1982).

[18] D.A. Bryan, R. Gerson, and H.E. Tomaschke, Appl. Phys. Lett. **44**, 847 (1984).

[19] D.K. Rice and L.G. De Shazer, Phys. Rev. **186**, 387 (1969).

[20] L. Kovacs, Zs. Szaller, I. Cravero, I. Földvari, and C. Zaldo, J. Chem. Phys. Solids **51**, 417 (1990).

[21]O.F. Schirmer, O. Thiemann, and M. Wöhlecke, J. Chem. Phys. Solids **52**, 185 (1991).
[22]S.C. Abrahams and P. Marsh, Acta Crystallogr. **45**, 805 (1984).
[23]H.J. Donnerberg, S.M. Tomlinson, and C.R.A. Catlow, J. Chem. Phys. Solids **52**, 201 (1991).
[24]F. Agulló-López and J.M. Cabrera, in *Properties of Lithium Niobate*, EMIS Data review Series No. 5, edited by INSPEC (EMIS, London, 1989), p. 8.